J. Fluid Mech. (1993), *vol.* 246, *pp.* 67–89

Acoustic behaviour of a liquid/vapour mixture in a standing-wave tube

By C. COSTE AND C. LAROCHE

ENS-LYON, Laboratoire de Physique, 46, Allee d'Italie, 69364 LYON Cedex 07, France

(Received 21 October 1991 and in revised form 23 March 1992)

We study the acoustic behaviour of a mixture of diethyl-ether bubbles and liquid, at small volume fraction of vapour, contained in a standing-wave tube. We give experimental evidence of the effect of the liquid/vapour phase transition on the positions and amplitudes of the resonances of the tube. The effective-medium theory, which properly describes the behaviour of liquid/gas mixtures, is shown to be inadequate. We find that theoretical studies which take the effect of the phase transition into account do agree with our experimental data.

1. Introduction

Sound propagation in liquid/gas mixtures is well documented both theoretically and experimentally; Commander & Prosperetti (1989) give an extensive review of experimental works with a heuristic exposition of the corresponding models, and the reader is referred to their review for references to the original studies.

At low acoustic frequency diphasic media are described with a good accuracy by the *effective-medium theory* (EMT) which considers that the liquid/gas mixture has an effective compressibility and an effective density which are the averages of the respective quantities in the two phases. Even at small gas volume fraction, this model predicts a very low speed of sound: in fact the density of the mixture is almost that of the liquid and its compressibility that of the gas, and the sound speed c_{eff} in the mixture is thus lower than both the speed in the pure liquid c_{l} and in the pure gas c_{g} (for example, in diethyl-ether $c_{\text{l}} \sim 1000$ m/s, $c_{\text{g}} \sim 200$ m/s and $c_{\text{eff}} \sim 100$ m/s at a volumic fraction of 0.35%).

The sound attenuation can be accounted for by considering the individual response of each bubble to the incident sound wave. A bubble response to the sound wave is that of a forced harmonic oscillator, the stiffness term being provided by the gas compressibility and the inertia term by the liquid density; the oscillations are damped by the surrounding liquid viscosity, by the gas thermal conduction and by the scattering† of sound, and this damping causes the attenuation of the sound wave.

When handling a liquid/vapour mixture instead of a liquid/gas one, one expects the effective compressibility of the mixture to be modified: the possibility of a phase transition allows a change in the volume of the bubbles due to the condensation/vapourization and not only to the compression of the vapour by the sound wave. The latent heat necessary for the phase transition should be transported by heat diffusion and this diffusive phenomenon is mainly responsible for the attentuation of the wave.

The first theoretical study including effects specific of liquid/vapour mixtures is

† Note that this is not, strictly speaking, a dissipative phenomenon but it removes energy from the incident direction of propagation and actually damps the sound wave.

that of Landau & Lifshitz (1959); they assumed thermodynamical liquid/vapour equilibrium everywhere in the mixture and their result is thus strictly valid only at zero frequency (see also Kieffer 1977). Later studies of Trammel (1962) and Nakoriakov *et al.* (1984) gave analytical expressions for the phase velocity and the attenuation for frequencies of the order of the bubble resonance frequency, but they failed to recover Landau & Lifshitz's result in the limit of zero frequency. Onuki (1991) solved this discrepancy using an effective-medium theory that incorporates the effect of the phase transition on the effective compressibility of the mixture; we call his model the *modified effective-medium theory* (MEMT). He recovered the results obtained by Trammel and Nakoriakov *et al.* in the high-frequency limit and Landau & Lifshitz's formula valid at zero frequency; moreover he showed that the crossover takes place when thermal interactions between the bubbles cannot be neglected. The main features of his model are in agreement with the rigorous result, valid at all frequencies, obtained by Boguslavskii (1978) for a solvable one-dimensional model. We should also mention the work by Mecredy & Hamilton (1972) and by Feldman, Nydick & Kokernak (1972) who failed to give an answer in closed form because they introduced an unknown phenomenological coefficient; Ardron & Duffey (1978) gave a numerical answer to the problem, in good agreement with the later results obtained by Onuki and by Nakoriakov *et al.*; lastly we mention the calculations of sound attenuation in liquid/vapour mixtures by Wang (1974) and Hsieh (1982), based on studies of vapour bubble oscillations by Finch & Neppiras (1973), Hsieh (1979) and Marston (1979).

To our knowledge only a few experimental studies have been carried out. Feldman *et al.* (1972) and Kokernak & Feldman (1972) give only qualitative results, and at frequencies too high for the phase transition to have any effect. Although our measurements were made at much lower frequencies, this is also the main defect of a previous work (Coste, Laroche & Fauve 1990). In the work by Mecredy, Wigdortz & Hamilton (1970), graphic representations of the phase velocity for a liquid/vapour and for a liquid/gas mixture are given but the measurements were carried only on a liquid/gas mixture (bubbles of nitrogen in water). As far as we know, all the works by Soviet scientists deal with nonlinear waves, and do not study the possible deficiency of the EMT for liquid/vapour mixtures in the linear regime (see Nakoriakov, Pokusaev & Shreiber 1980; Borisov *et al.* 1983; Kutateladze, Nakoriakov & Borisov 1987 and Nigmatulin, Khabeev & Zuong Ngok Hai 1988; see also the book by Nigmatulin 1991).

The organization of this paper is as follows: first we briefly summarize the results of the two theoretical models (§2). Then we describe our experimental set-up, the method of measurements for the volume fraction and the acoustic behaviour of our system, in order to compare the predictions of the models with the experimental results (§3). Next we describe the various measurements that we have made, and show a clear discrepancy with the predictions of the EMT; on the other hand, those of the MEMT do agree with our experimental results (§4). In the last section we summarize our results and extensively discuss their main limitation, that is the unavoidable polydispersity of the bubble population in our experiments (§5).

2. The models

In this Section, we give a brief review of the theoretical models of interest. Although the works we quote are often much more general, we restrict the hypothesis because of our experimental conditions: we consider only sound waves of small

Definition	Symbol	Value	Unit	Temperature
Latent heat of vapourization	L_v	380×10^3	J kg^{-1}	34.5 °C
Heat capacity (liq.)	C_p^l	2.26×10^3	J kg^{-1} K^{-1}	30 °C
Heat capacity (vap.)	C_p^g	1.42×10^3	J kg^{-1} K^{-1}	30 °C
Density (liq.)	ρ_l	736 (713)	kg m^{-3}	0 °C (25 °C)
Density (vap.)	ρ_g	3.3	kg m^{-3}	34.5 °C
Sound velocity (liq.)	c_l	1030	m s^{-1}	15 °C
Sound velocity (vap.)	c_g	187	m s^{-1}	34.5 °C
Surface tension	σ	17×10^{-3}	N m^{-1}	20 °C
Viscosity (liq.)	μ_l	2.2×10^{-4}	kg m^{-1} s^{-1}	25 °C
Viscosity (vaq.)	μ_g	7.5×10^{-6}	kg m^{-1} s^{-1}	25 °C
Thermal conductivity (liq.)	λ_l	0.138	J s^{-1} m^{-1} K^{-1}	30 °C
Thermal diffusivity (liq.)	D_l	8.3×10^{-8}	m^2 s	30 °C

TABLE 1. The numerical values of the mechanical and thermal properties of diethyl-ether used in the experiments, for both the liquid (liq.) and vapour (vap.) phases. The definitions are listed in the first column, the symbols we use in the text in the second one, the respective value and unit in the third and fourth ones; in the last column we quote the temperature at which the measurements are done. Those values (with the exception of c_l, which we measured) are taken from the *Handbook of Chemistry and Physics*, The Chemical Rubber Publishing Company, Cleveland, Ohio.

amplitude so that we are in the *linear regime* and of frequency much lower than the resonance frequency of the individual bubbles. We also neglect *all effects due to surface tension* because they are relevant only for very minute bubbles (with a radius typically smaller than a few μm) and we consider only the case of a *small volume fraction of gas (or vapour)*. The last assumption we make is the following logical requirement for the homogenization of the mixture: the bubble sizes and the mean distance between them should be small compared to the wavelength; it is always the case in our experiments, and could be violated only at very high frequency (typically 10^6 Hz for a bubble with a 1 mm radius).

In our experiments, the working liquid is diethyl-ether; the mechanical and thermal properties required in the calculations are listed in table 1.

2.1. *The effective-medium theory*

The simplest picture of a liquid/gas diphasic mixture is that of an effective medium, the density and compressibility of which being the averages of the respective quantities in the gas and liquid phases (Mallock 1910). Let f be the volume fraction of gas, that is

$$f \equiv V_g/(V_g + V_l).$$

We define the average of a quantity X by $\langle X \rangle \equiv (1-f)X_l + fX_g$ and we thus get the following expression for the sound velocity in the mixture:

$$c_{\text{eff}}^2 = \frac{1}{\langle \rho \rangle \langle \chi \rangle} = \frac{\rho_l \rho_g c_l^2 c_g^2}{[\rho_l(1-f)+\rho_g f][\rho_g c_g^2(1-f)+\rho_l c_l^2 f]}, \tag{2.1}$$

where the averaged density $\langle \rho \rangle$ and averaged compressibility $\langle \chi \rangle$ of the mixture are expressed on the right-hand side in terms of the density ρ_i and of the sound velocity c_i for each phase i. In this simple model, the mixture is characterized only by the mean quantity f; thus a detailed statistical knowledge of the bubble population is unnecessary. In turn the simple formula (2.1) fails to account for the sound wave attenuation. When the volume fraction of gas is not too low, so that

$$\rho_g c_g^2(1-f) \ll \rho_l c_l^2 f,$$

using $\rho_l(1-f) \gg \rho_g f$ and the well-known expression $c_g^2 = \gamma p_0/\rho_g$, where p_0 is the ambient pressure and γ the adiabatic exponent of the gas, which is supposed to be perfect, we obtain the following useful approximation:

$$c_{\text{eff}}^2 \approx \gamma p_0/(\rho_l f). \tag{2.2}$$

To introduce dissipative phenomena it is necessary to study the individual behaviour of each bubble. In the linear regime, a bubble in a sound field can be described as a forced harmonic oscillator, the stiffness of which is related to the compressibility of the gas and the inertia term to the density of the liquid; its resonance pulsation ω_r is given by (Minnaert 1933)

$$\omega_r^2 \equiv 3\gamma p_0/(\rho_l R_0^2), \tag{2.3}$$

where R_0 is the equilibrium radius of the bubble. The next step is to describe the scattering of a sound wave by the set of bubbles; the problem has been solved by Cartensen & Foldy (1947) who found the (complex) propagation constant to be

$$\frac{k^2}{\omega^2} = \frac{1}{c_l^2} + \frac{\rho_l f}{\gamma p_0} \frac{1}{1-(\omega^2/\omega_r^2) - i\delta(\omega)}, \tag{2.4}$$

where k is the wavenumber and ω the pulsation. The phase velocity c_ϕ and the attenuation α_ϕ are

$$c_\phi \equiv \omega/Re[k(\omega)], \quad \alpha_\phi \equiv \text{Im}[k(\omega)]. \tag{2.5}$$

The expression (2.4) exhibits both dispersion and attenuation through the dimensionless damping constant δ. The dispersion is a physical consequence of the fact that a natural timescale (the oscillation period of a bubble) has appeared in the problem; another way of seeing this is to remember that attenuation and dispersion are related to each other by the Kramers–Kronig relations (for applications to bubbly diphasic media see Temkin 1990). Devin (1959) showed that the damping is due to the viscous dissipation at the liquid/gas boundary (δ_{vis}), to the re-radiation of sound by the bubble (δ_{rad}) and to the thermal diffusion in the gas (δ_{th}). The source of this last effect is the polytropic behaviour of the gas, which generates a hysteresis effect between pressure and volume variation and thus damps the sound wave; in fact the gas behaves isothermally near the boundary because of the large specific heat of the liquid and almost adiabatically in the centre of the bubble, and its global behaviour is actually polytropic. The damping constant is the sum of the following three expressions:

$$\delta_{\text{vis}} = \frac{4\mu_l \omega}{3\gamma p_0}, \quad \delta_{\text{rad}} = \frac{\omega R_0}{c_l}\left(\frac{\omega}{\omega_r}\right)^2, \quad \delta_{\text{th}} = \frac{3}{2}\frac{\gamma-1}{R_0}\left(\frac{2D_g}{\omega}\right)^{\frac{1}{2}}, \tag{2.6}$$

where we have introduced the viscosity of the liquid μ_l and the thermal diffusivity of the gas D_g; the bubbles are supposed to be monodispersed since only one resonance pulsation, ω_r, appears. The validity of (2.4) and (2.6) is well established experimentally for liquid/gas mixtures, at least at low frequency; a critical review of the various experimental works as well as a heuristic derivation of (2.4) are to be found in the review by Commander & Prosperetti (1989).

The problem of thermal damping has been reconsidered recently by Prosperetti (1977, 1991); he gave an intricate analytical expression for δ_{th} which is valid at any frequency and he showed that (2.6) is recoveed in the high-frequency limit. The natural timescale here is the characteristic heat diffusion time in the bubble, and the

high-frequency limit is reached when the dimensionless parameter $R_0(2\omega/D_g)^{\frac{1}{2}} \geqslant 20$. For a frequency about 10 Hz, we get† $R_0(2\omega/D_g)^{\frac{1}{2}} \approx 7.5$ and the approximation (2.6) gives a slight overestimate of the thermal damping (see figure 2 of Prosperetti 1991).

The resonance frequency of a 1 mm radius vapour bubble in diethyl-ether is $\omega_r/2\pi \approx 3.9$ kHz, and for an acoustical frequency of 100 Hz the orders of magnitude of the various damping constants are

$$\delta_{\rm vis} \approx 1.3\times10^{-6}; \quad \delta_{\rm rad} \approx 6.2\times10^{-4}; \quad \delta_{\rm th} \approx 6.2\times10^{-2}.$$

Thus the thermal damping is widely predominant but remains small; a good approximation of (2.4) at low frequency (i.e. much less than the bubble resonance frequency) is

$$k = (\omega/c_{\rm eff})\,[1+{\rm i}\tfrac{1}{2}\delta_{\rm th}(\omega)], \tag{2.7}$$

where $c_{\rm eff}$ is introduced with the help of (2.2). The latter expression is used in §4 to compute the predictions of the EMT.

2.2. *The modified effective-medium theory*

Consider a vapour bubble in (unstable) equilibrium with the surrounding liquid. Because of the sound wave, the pressure is no longer at its equilibrium value, and the bubble's volume decreases or increases depending on whether some vapour is condensed or some liquid is vaporized. Therefore a vapour bubble changes its volume not only by the compression/dilatation of the vapour, but also because of the mass transfer between the two phases. Consequently the *effective compressibility* of the liquid/vapour mixture, and thus its acoustic properties, are different from that of the liquid/gas mixture.

This new mechanism acts only at low frequency because the latent heat of vaporization must be provided to (or removed from) the interface by the surrounding liquid; it is clear that, at least at low volume fraction of gas, the liquid plays the role of a heat bath and that the kinetic of the process is limited by the conduction of heat in the liquid. A typical time appears naturally; it is dimensionally made up of the thermal diffusivity of the liquid D_1, and the typical lengthscale of the system R_0, and thus has order of magnitude $\sim R_0^2/D_1$. The existence of this timescale makes the speed of sound *dispersive*, in contrast to $c_{\rm eff}$ (see (2.1)). There is also an additional attenuation process because the diffusive process of heat transfer is necessary for the mass transfer to occur.

A theory for the liquid/vapour mixtures has been given recently by Nakoriakov *et al.* (1984) and Onuki (1991); the expression of the propagation constant is found to be

$$k = \frac{\omega}{c_{\rm eff}}\left[1+\frac{m}{(2\omega\tau_1)^{\frac{1}{2}}}(1+{\rm i})\right]^{\frac{1}{2}}. \tag{2.8}$$

The characteristic time of diffusion over a bubble $\tau_1 \equiv R_0^2/D_1$ appears here; the parameter m is given by

$$m \equiv 3\gamma p_0 \rho_1 C_p^{\rm l} T_0/(\rho_{\rm g}^2 L_{\rm v}^2) \tag{2.9}$$

It expresses the thermal properties of the medium: $L_{\rm v}$ is the latent heat of vaporization, T_0 the equilibrium temperature and $C_p^{\rm l}$ the specific heat at constant pressure of the liquid. The physical meaning of m can be shown by rewriting it in a

† We estimate the thermal diffusivity of the vapour, $D_{\rm G}$, with the help of the well known formula $(\rho_{\rm g} D_{\rm g})/\mu_{\rm g} \approx 1$.

different way. If we assume the liquid/vapour interface to be in thermodynamic equilibrium, the Clapeyron–Clausius condition $T_0/(\rho_g L_v) = (\mathrm{d}T/\mathrm{d}p)_{eq}$ is satisfied; we also assume that the vapour behaves adiabatically, so that $\mathrm{d}p/\mathrm{d}\rho_g = \gamma p_0/\rho_g$, and we obtain

$$m = \underbrace{3\rho_l C_p^l \,\mathrm{d}T}_{Q_l} \underbrace{\frac{1}{L_v \,\mathrm{d}\rho_g}}_{Q_g}$$

Thus, we see that m is the ratio of the heat Q_l stored by the liquid which undergoes a temperature variation $\mathrm{d}T$ to the heat Q_g necessary to the phase transition. If Q_l is larger thn Q_g, m is large and the speed of sound is much lower than c_{eff}; this corresponds to the fact that if the liquid stores heat well the vaporization is easier and the effective compressibility of the medium larger, in agreement with the simple physical picture.

It is important to discuss the range of validity of (2.8). First we note that the frequency is supposed to be much lower than the resonance frequency of the bubbles, (2.3); indeed it has been shown by Nakoriakov *et al.* (1984) that near the resonance frequency (2.3) a liquid/vapour mixture behaves like a liquid/gas one to a very good approximation: at such a frequency the pressure variations are too fast to allow heat transfers between the two phases. It is thus consistent that the high-frequency limit of (2.8) gives c_{eff} as the sound velocity, but one has to keep in mind that this 'high-frequency limit' is actually an intermediate one, much higher than the typical thermal frequency but much lower than the bubble resonance frequency.

In the limit of very low frequencies (in a sense to be made precise later), (2.8) gives rather unphysical results: taking the limit $\omega \to 0$ gives $c_\phi = 0$. At zero frequency the mixture is in thermal equilibrium and one must recover the result obtained by Landau & Lifshitz (1959): they found a null attenuation, and a phase velocity c_{eq} which is much smaller than c_{eff}. Onuki (1991) showed that at low frequency the temperature field around each bubble extends too far (with respect to the mean bubble distance), so that it is impossible to neglect thermal interactions between the bubbles, as it is explicitly done to obtain (2.8); Onuki gives an analytic expression for the complex constant of propagation which is valid in all the frequency range of interest:

$$k^2 = \frac{\omega^2}{c_{eff}^2} + \frac{\omega^2}{c_{eq}^2} \frac{3f[1+(\mathrm{i}\omega\tau_l)^{\frac{1}{2}}]}{\mathrm{i}\omega\tau_l + 3f[1+(\mathrm{i}\omega\tau_l)^{\frac{1}{2}}]}. \tag{2.10}$$

In the zero-frequency limit, one recovers $c_{eq}$for the phase velocity, and the asymptotic behaviour of the attenuation is

$$\alpha_\phi \propto \omega^2 R_0^2/(D_l c_{eq}), \tag{2.11}$$

which respects the physical requirement of null attenuation at null frequency. The same result have been obtained by Bogusslavski (1978) for an exactly solvable one-dimensional model, the proportionality constant being of course different (and the radius R_0 being replaced by the thickness of the vapour layer).

The most interesting feature of (2.10) is that it predicts a resonant attenuation of sound waves at a very low frequency, depending on τ_l but also on the volume fraction f (see figure 2*b* of Onuki's paper). This reflects the fact that when the frequency goes to zero the bubbles are thermally in interaction: the typical time for heat diffusion is no longer $\tau_l = R_0^2/D_l$ but rather $\tau_l' \equiv l^2/D_l$ where l is the mean distance between the bubbles. A rough estimate of τ_l' is easy to obtain. Let n be the number of bubbles

(supposed all of radius R_0) per unit volume. We have $f = \frac{4}{3}\pi R_0^3 n$ so that $n \propto f/R_0^3$; now the mean distance between the bubbles is $l \propto n^{-\frac{1}{3}} \propto R_0 f^{-\frac{1}{3}}$ and we obtain

$$\tau_1' \propto R_0^2/(f^{\frac{2}{3}} D_1) = \tau_1/f^{\frac{2}{3}}. \tag{2.12}$$

The inverse of this time gives an estimate of the resonant absorption frequency, in agreement with the exact value given by (2.10): for volume fractions of 0.15, 0.05 and 0.005 the attenuation is maximum at a frequency $1/(2\pi\tau_1)$, $0.1/(2\pi\tau_1)$ and $0.01/(2\pi\tau_1)$ respectively (the values are taken from figure 2*b* of Onuki's paper), while our estimate gives $0.3/(2\pi\tau_1)$, $0.14/(2\pi\tau_1)$ and $0.03/(2\pi\tau_1)$ respectively.

2.3. *Experimental test*

In order to observe significant effects due to mass transfer between the liquid and its vapour it is necessary to work at sufficiently low frequency, typically a few tens of Hz. In an earlier study (Coste *et al.* 1990) we never used a sound wave of frequency below 250 Hz and were unable to see any discrepancy between our experiments and the EMT. The addition of a Helmholtz resonator at the end of our standing wave apparatus (see below for further details of the experimental facilities) allows us to lower the frequency down to 2 Hz, and to discriminate between the behaviours predicted by (2.7) and (2.8).

On the other hand, the bubble radius R_0 is of order 1 mm, the typical diffusion time τ_1 of order 10 s and the volume fraction is about 10^{-3} in our experiments; the frequency of resonant attenuation predicted by Onuki (1991) is extremely low in those conditions, typically a few mHz (see figure 2 of Onuki's paper, or the order of magnitude given by (2.12)). Thus, we did not observe this regime, nor the equilibrium phase velocity c_{eq}.

3. Experimental procedures

3.1. *Experimental set-up*

The experimental set-up is shown in figure 1. It consists of a set of two coaxial glass tubes terminated by a Helmholtz resonator. The total length of the tubes is 2 m, the inner tube is 20 mm ID and the outer one 32 mm ID. The resonator is a cylinder made of 5 mm thick Pyrex, its height is 295 mm and its diameter 150 mm so that its volume is approximately 5 l; the copper part which joins the resonator to the tube is hollow and 5 mm thick. In the space between the tubes there are two independent circulations of water, for thermal regulation: the temperature of the upper part of the tube is held constant at 5 °C, that of the lower part at 15 °C (± 0.1 °C); note also that the resonator is held at the same temperature as the lower part of the tube: there is a circulation of water in the bigger tank in which the resonator is contained and in the hollow piece of copper.

The working liquid is diethyl-ether and is contained in the inner tube. Bubbles of vapour are produced in the lower part of the tube with the help of four resisting wires; these 50 cm long wires of total resistance 11Ω are heated by the current produced by a stabilized d.c. power supply; the experiments are carried with heating intensities in the range 0–4 A. Bubbles appear on the wires, then rise in the liquid; since the temperature of the upper part of the tube is much lower than diethyl-ether boiling point (34 °C), they condensate very rapidly after leaving the heated part of the tube.

Acoustic waves are generated by a piston held on a electromechanical vibration exciter at the top of the tube and they are detected by two piezoelectrical

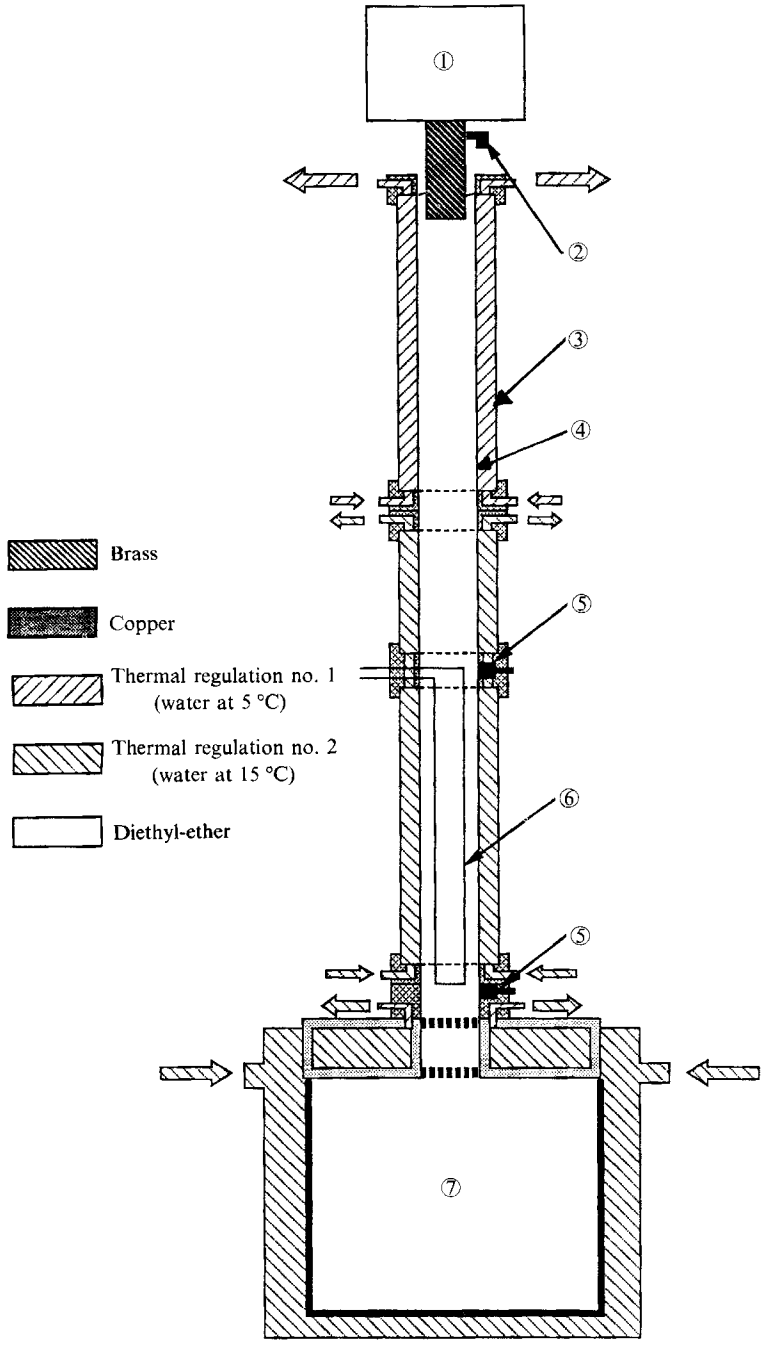

FIGURE 1. Sketch of the experimental apparatus; (1) electromechanical vibration exciter, (2) piezoelectric accelerometer, (3) outer Pyrex tube, (4) inner Pyrex tube, (5) piezoelectric hydrophones, (6) heating wires, (7) Helmholtz resonator.

transducers: one is located at the bottom of the tube, at the junction with the resonator, and the other one is 585 mm higher. A minature piezoelectrical accelerometer is also fixed on the piston in order to compare its mechanical response to the electrical excitation.

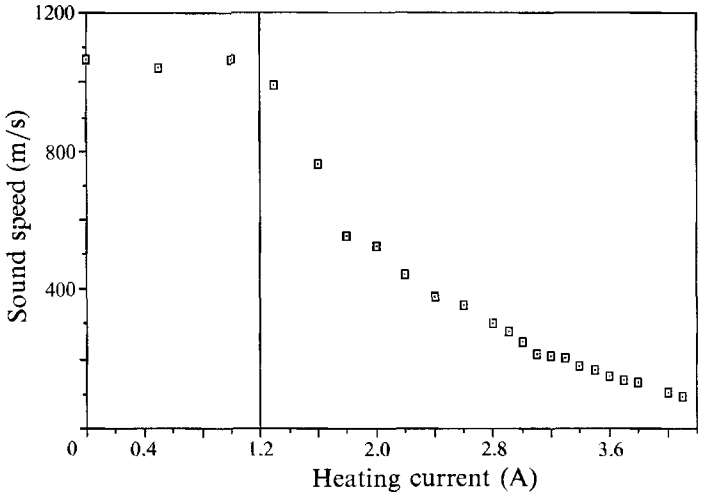

FIGURE 2. Plot of the speed of sound from pulse flight time measurements versus the heating current. This plot serves to determine the intensity I_0 at which bubbling begins, as indicated by the vertical line on the figure. The speed of sound is always a decreasing function of the heating current because the mean temperature of the lower part of the tube increases; this is the change of slope which gives the value of I_0, 1.2A in our experiments.

Two kind of measurements are made, both with low-amplitude pressure perturbations. First the vibration exciter is driven by one-period sine pulses, and the velocity is determined by the flight time between the two detectors. Then we study the standing-wave behaviour of the tube. A first method is to store the pressure signal given by the two transducers on an IBM PC, for frequency excitations which are separated by 0.1 Hz steps and range mostly from 2 to 300 Hz. A one minute's averaging is performed for each measurement. Another approach is to study the frequency response of the system with the help of a spectrum analyser; either we supply the vibration exciter with white noise, or we use the fact that the surrounding noise is enough to excite the lowest resonances of the tube.

3.2. *Measurements of the volume fraction of vapour*

The mean volume fraction is determined by the change in the height of the liquid column when bubbling begins. To this end we use a cathetometer to mark the upper level of liquid; the precision is about 0.05 mm. Of course we have to take into account the dilatation due to the heating current; since a phase transition takes place at constant temperature we assume that, after the first bubble has appeared for a given value I_0 of the heating current, the changes in height for $I > I_0$ are only due to the increasing volume of vapour. To determine I_0, the easiest and most precise way is to plot the velocity given by the flight time measurements versus the intensity; this is done in figure 2, so that we get the abscissa I_0 corresponding to the zero volume fraction. The volume fraction is then deduced from the fact that its value is equal to zero for $I = I_0$. Such measurements are not very precise because a great importance is given to the points at low intensity, for which the changes in height are the most difficult to measure.

However we have verified the values of f by comparison between the predictions of EMT and the velocity of sound given by the measurements of the flight times of the pulses; the results are shown on figure 3. The duration of the pulses is about

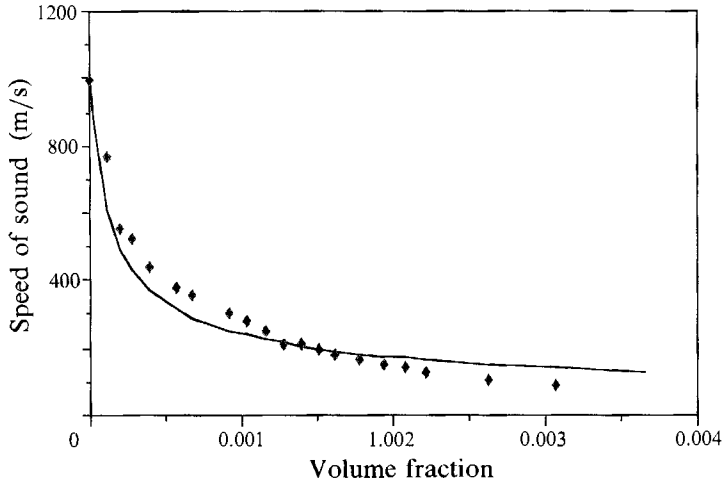

FIGURE 3. Plot of the speed of sound from pulse flight time measurements versus the volume fraction (points) and comparison with the prediction of the EMT (solid line).

10^{-3} s, too short a time for effects due to the liquid/vapour transition to be important, and thus the sound velocity should be given by (2.1). Actually the experimental points are very close to the theoretical values, which confirms the measurements of f. In fact, according to (2.8), the volume fraction enters the MEMT only through the coefficient c_{eff}. Subsequently, we use directly the experimental values of c_{eff} in equations (2.7) and (2.8) for the calculations in §4.

A limitation of our experiments is that we have no statistical information on the bubble population. On one hand, from a purely experimental point of view it is difficult to use optical methods (e.g. macrophotography) because there are two different fluids separated by two solid cylindrical walls. On the other hand, local photographs are of little interest because a bubble of vapour is never at equilibrium and its radius R_0 evolves during the ascension. We thus analyse our data (see §4) with R_0 taken as a parameter and treat the mixture as if it were monodisperse; we discuss this point at length in §5 below and we give arguments which explain why the polydispersity has no dramatic effect.

3.3. *Standing-wave behaviour in a tube*

Consider an enclosed mechanical system, the input to which are waves generated by an appropriate vibration exciter. If the excitation force is $F = F_0 e^{i\omega t}$ the input mechanical impedance Z_{m0} is defined by $Z_{m0} = F/u_0$ where u_0 is the speed at the application point of the force. In the absence of damping Z_{m0} is pure imaginary; since the force is finite, when $Z_{m0} = 0$ the speed u_0 is infinite: this is the condition of *mechanical resonance*. The generalization to the dissipative case is not difficult (see e.g. Kinsler *et al.* 1982, p. 66) and a resonance of the system is defined by the fact that *the imaginary part of the input impedance is zero.*

We use this definition to calculate the resonance frequency of our system. We take the following model: we divide the tube in two parts (see figure 1), the upper one (part 1) between abcissa $x = 0$ and $x = l$ contains the pure liquid at a temperature of 5 °C, the lower one (part 2) between $x = l$ and $x = L$ contains the diphasic mixture and is ended by the terminal impedance Z_L. Of course this is an idealization because the boundary between the two fluids has actually a finite length, but an estimate of

this length is easily obtained, showing that it is negligible compared to the other relevant lengths of the problem. The collapse of a vapour bubble is a difficult problem (see e.g. Plesset & Prosperetti 1977) but a vapour bubble of radius 1 mm is sufficiently big for its growth to be described by the asymptotic formula of Plesset & Zwick (1954): $R(t) = R_0 + C_1 t^{\frac{1}{2}}$, where $C_1 \equiv 2\lambda_1(T_{eb} - T_0)/(L\rho_g D_1)$. This formula can be applied to the beginning of the collapse, but not to the later stage, when the size of the bubble becomes smaller than the typical length of heat diffusion in the liquid; but we may suppose that it gives an upper limit of the collapse time Δt_c, that is $\Delta t_c \approx R_0^2/C_1^2$. On the other hand, under the action of buoyancy and viscous forces, the bubble has a limit speed v given by: $v = C_2 R^2(t)$ where $C_2 \equiv \rho_l g/(3\mu_l)$, g being the acceleration due to gravity. Making the rather crude assumption that during the collapse the bubble has a speed always equal to its limit value, we get the following estimate for the length l_c on which the collapse takes place:

$$l_c \approx \int_0^{R_0^2/C_1^2} C_2(R_0 - C_1 t^{\frac{1}{2}})^2 \, dt = \frac{C_2 R_0^4}{6C_1^2}.$$

The temperature of the upper part of the tube is 5 °C so that $T_{eb} - T_0 \approx 29$ °C and we thus obtain $l_c \approx 4$ mm; this length is much smaller than the wavelength and the length of each part of the tube, thus justifying the assumption of discontinuous properties of the fluid at the junction between the two parts of the tube.

We also neglect all dissipative effects due to viscous damping and to heat exchanges between the fluid and the walls. Those phenomena are well known and the expression for the attenuation is (see e.g., Morse & Ingard 1986, p. 519)

$$\alpha_\phi = \frac{\omega^{\frac{1}{2}}}{\sqrt{2}ac}\left[(\gamma - 1)D_1^{\frac{1}{2}} + \left(\frac{\mu_l}{\rho_l}\right)^{\frac{1}{2}}\right], \tag{3.1}$$

where a is the radius of the tube and c the speed of sound in the fluid. For a frequency $\omega/2\pi = 100$ Hz, a bubble radius $R_0 = 1$ mm and an effective velocity $c_{eff} = 200$ m/s, numerical estimations using (3.1), in the case of the pure fluid and (2.6) and (2.5) for the two models of liquid/vapour mixtures give the following values for the attenuation:

$$\alpha_\phi \approx 9 \times 10^{-4} \text{ m}^{-1}, \quad \text{pure fluid},$$
$$\alpha_\phi \approx 9 \times 10^{-2} \text{ m}^{-1}, \quad \text{EMT},$$
$$\alpha_\phi \approx 1 \text{ m}^{-1}, \quad \text{MEMT}.$$

Thus the attenuation in the part of the tube filled with pure fluid, due to viscous damping and heat exchange at the walls, is much smaller than the attenuation predicted either by the MEMT or the EMT without taking the walls into account. Note also that even at a relatively high frequency (compared to the timescale of the condensation/vaporization process) the MEMT predicts an attenuation much higher than the one given by the EMT.

We define the acoustic pressure in each part of the tube by

$$P_1(x) = A_1 e^{-ik_1 x} + B_1 e^{+ik_1 x}; \quad P_2(x) = A_2 e^{-i\tilde{k}_2 x} + B_1 e^{+i\tilde{k}_2 x}, \tag{3.2}$$

where we drop the factor $e^{i\omega t}$ and x is the distance from the tube input; the notation $\tilde{k}_2$ expresses the complex nature of the constant of propagation in part 2 of the tube, whereas dissipation is neglected in part 1, so that k_1 is real. Let ρ_i and c_i respectively denote the density and the speed of sound in the part i of the tube, and S the area of its section.

At any point x the mechanical impedance is $Sp(x)/u(x)$ and is obtained in a very simple way from (3.2) together with the formula $u(x,t) = -(1/\rho_1)\int(\partial p/\partial x)\,dt$. The continuity of the acoustic pressure and of the normal velocity at the junction between the two parts of the tube and at the entrance of the Helmholtz resonator is thus most easily expressed by the continuity of the complex mechanical impedance.

The continuity of the mechanical impedance at $x = L$ gives the following equation:

$$Z_L = \rho_2 \frac{\omega}{\tilde{k}_2} S \frac{A_2 e^{-i\tilde{k}_2 L} + B_2 e^{+i\tilde{k}_2 L}}{A_2 e^{-i\tilde{k}_2 L} - B_2 e^{+i\tilde{k}_2 L}}, \tag{3.3}$$

and the continuity of the acoustic impedance at the junction between the two parts of the tube, at $x = l$, is expressed by

$$\frac{A_1 e^{-ik_1 l} + B_1 e^{+ik_1 l}}{A_1 e^{-ik_1 l} - B_1 e^{+ik_1 l}} = \frac{\rho_2}{\rho_1} \frac{\omega}{\tilde{k}_2 c_1} \frac{A_2 e^{-i\tilde{k}_2 l} + B_2 e^{+i\tilde{k}_2 l}}{A_2 e^{-i\tilde{k}_2 l} - B_2 e^{+i\tilde{k}_2 l}} \equiv R. \tag{3.4}$$

Lastly, the condition of resonance may be written:

$$\mathrm{Im}\left(\frac{A_1 + B_1}{A_1 - B_1}\right) = 0, \tag{3.5}$$

where $\mathrm{Im}(C)$ stands for the imaginary part of the complex number C. One should remark that in this last equation, the mechanical impedance of the vibration exciter is neglected; this approximation is justified by our experiments when the tube is filled with pure fluid (that is, no heating and thus no bubbles). The measurements are reported in Coste (1991). Equations (3.3), (3.4) and (3.5) allow the numerical calculation of the resonances but it is convenient to rewrite them.

We define t by $\tilde{k}_2 = (\omega/c_{\mathrm{eff}})\,t$; t is a corrective factor to the simplest version of the EMT (see (2.1)) and its expression is given by (2.7) when the bubbly liquid is described by the EMT and (2.8) when it is described by the MEMT. For diethyl-ether under the experimental conditions given in §3.1 it is

$$t = \left(1 + \frac{9.76}{R_0 \nu^{\frac{1}{2}}} + i\frac{9.76}{R_0 \nu^{\frac{1}{2}}}\right)^{\frac{1}{2}} \quad \text{(MEMT)}, \tag{3.6a}$$

$$t = 1 + i\frac{0.31}{R_0 \nu^{\frac{1}{2}}} \quad \text{(EMT)}, \tag{3.6b}$$

where ν is the frequency in Hz and R_0 the radius of the bubbles (for a monodisperse population) in mm. We also define the dimensionless impedance z and z_L by

$$z \equiv \frac{\tilde{k}_2 Z_L}{\rho_2 \omega S} = \frac{Z_L t}{\rho_2 c_{\mathrm{eff}} S} \equiv i z_L \frac{c_1}{c_{\mathrm{eff}}} t, \tag{3.7}$$

z_L is the dimensionless terminal impedance; the tube is terminated by a Helmhotz resonator, a very simple acoustical system consisting of a neck connected to a cavity. This set behaves like a harmonic oscillator if each of its dimension is much less than the wavelength: the mass element is provided by the fluid contained in the neck, whereas the stiffness element is related to the compressibility of the fluid in the cavity (see e.g. Kinsler *et al.* 1982, p. 225); it is used here to lower the resonance frequency of the tube. The functional form of z_L is that of an harmonic oscillator, i.e.

$z_L = \mathrm{i}(\alpha_L \nu - \beta_L/\nu)$; the inductive ($\alpha_L = 2.45 \times 10^{-3}$) and capacitive ($\beta_L = 4.38$) terms are calculated elsewhere and are consistent with precise measurements when the tube is filled only with liquid (Coste 1991).

Lastly, we introduce a coefficient Y by

$$B_1 \equiv Y A_1. \tag{3.8}$$

With those definitions, the system of equations which gives the resonance frequencies of the tube has the following form:

$$\left.\begin{aligned} R &= \frac{\rho_2 c_{\mathrm{eff}}}{\rho_1 c_1} \frac{(z+1)\,\mathrm{e}^{\mathrm{i}\tilde{k}_2(L-l)} + (z-1)\,\mathrm{e}^{-\mathrm{i}\tilde{k}_2(L-l)}}{(z+1)\,\mathrm{e}^{\mathrm{i}\tilde{k}_2(L-l)} - (z-1)\,\mathrm{e}^{-\mathrm{i}\tilde{k}_2(L-l)}}, \\ Y &= \mathrm{e}^{-2\mathrm{i}k_1 l} R - 1/(R+1), \\ \mathrm{Im}\,(Y) &= 0. \end{aligned}\right\} \tag{3.9}$$

The numerical resolution of this system allows the calculation of the resonance frequencies of the tube for the two models.

The resonance frequency is not the only relevant information given by an experimental resonance curve; the maximum pressure amplitude or the width of the curve are also easily measured and are not given by (3.9). Moreover, as will be shown in §4.3, there exist maxima of the pressure which are not 'true' resonances, that is which do not correspond to the annulation of the imaginary part of the input impedance. In order to compare such information with the calculations, we also need an expression for the pressure at a given point of the tube as a function of the frequency. It is straightforward to obtain from (3.2) and (3.8) the pressure amplitude $P_l(\nu)$ at the distance l from the tube input, where the upper detector is located:

$$P_l(\nu) = P_0 \left| \frac{\mathrm{e}^{-\mathrm{i}k_1 l} + Y\,\mathrm{e}^{\mathrm{i}k_1 l}}{1+Y} \right| \tag{3.10}$$

where P_0 is the pressure at the tube input and $|C|$ stands for the modulus of the complex number C.

4. Results

Our apparatus does not allow direct measurements of the attenuation and the phase velocity versus the frequency of the sound wave. We study the response of the apparatus as a function of the frequency of the input excitation, and how it evolves with the volume fraction of vapour. It depends directly on the attenuation and phase velocity of the wave in the bubbly part of the tube, and the results of the preceeding section allow direct comparison between the experimental features of the resonance curves and their theoretical values. We study the positions of the two first resonances of the tube (see §§4.1 and 4.2 below), which are related to both the attenuation and phase velocity of the wave, the width of the first resonance (see §4.2) and the relative amplitude of the two resonances (see §4.4), these last properties depending mostly on the attenuation.

4.1. *Position of the first resonance*

The evolution of the first resonance with the volume fraction f is displayed in figure 4; it shows some very intuitive features: the resonance frequency becomes lower when f increases, which indicates that the speed of sound is a decreasing function of f, and there is also a regular widening of the curves accounting for the increase of the

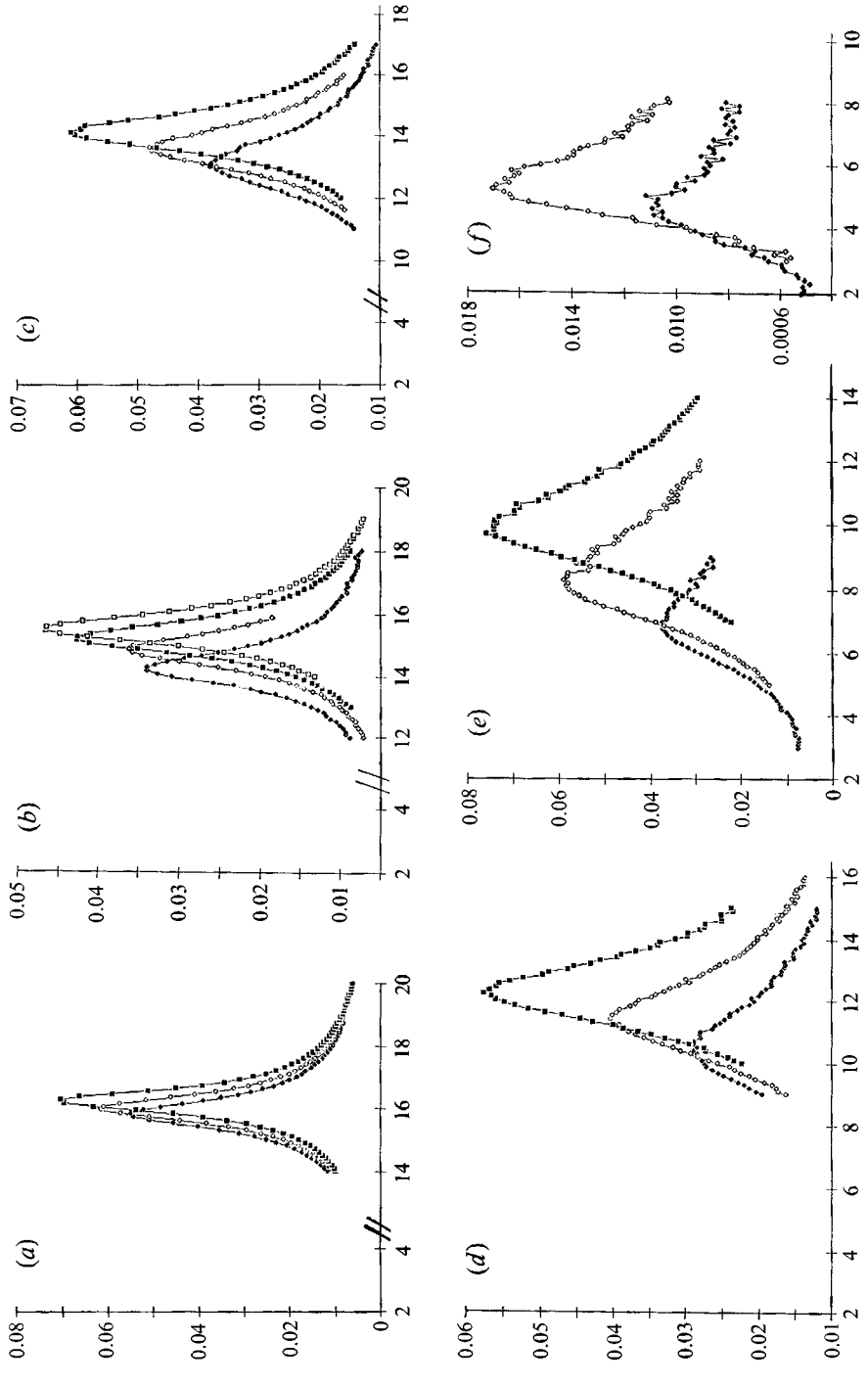

FIGURE 4. Experimental resonance curves for the first resonance (the fundamental frequency) of the tube; the ordinate is the amplitude of the pressure signal in arbitrary units and the abcissa is the frequency in Hz. Each part (*a–f*) is a series of curves with the same peak/peak voltage amplitude on the vibration exciter; if the amplitude of series (*a*) is taken as unity, the amplitude is 1 for (*b*), 2 for (*c*) and (*d*), 3 for (*e*) and 4 for series (*f*). The volume fractions f for each curve are as follows: (*a*) 0, 2.4×10^{-5} and 1.1×10^{-4}; (*b*) 2.0×10^{-4}, 2.7×10^{-4}, 4.0×10^{-4} and 5.7×10^{-4}; (*c*) 6.8×10^{-4}, 9.2×10^{-4} and 1.2×10^{-3}; (*d*) 1.4×10^{-3}, 1.6×10^{-3} and 1.9×10^{-3}; (*e*) 2.1×10^{-3}, 2.2×10^{-3} and 2.4×10^{-3}; (*f*) 2.6×10^{-3} and 3.1×10^{-3}. The resonance frequency decreases with the volume fraction.

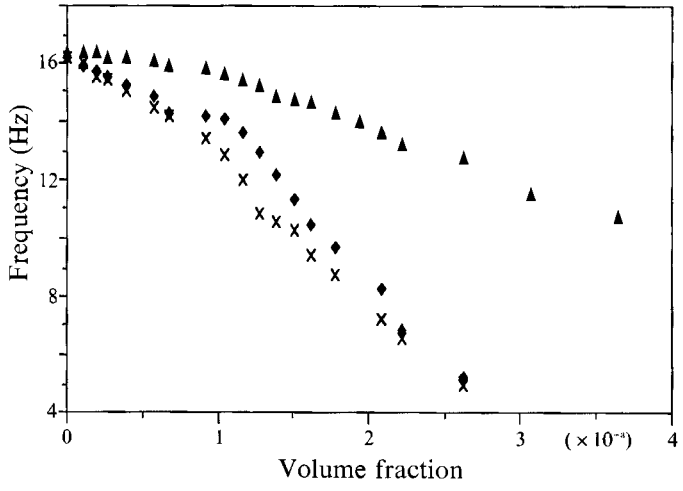

FIGURE 5. Evolution of the first resonance frequency with the volume fraction. A comparison is made between the experimental values (◆), the predictions of EMT (▲) and those of the MEMT (×).

damping. For a quantitative study one must use (3.9) and compare the prediction of EMT and MEMT to the measurements; the evolution of the positions of the resonance frequencies is studied in this subsection, whereas the next subsection is concerned with the evolution of the width of the curves.

The radius of the bubbles is taken to be 1 mm. This value is consistent with direct observation but is necessarily an approximation of the actual distribution; a full discussion is presented in §5. The result of the comparison is displayed in figure 5. The discrepancy between the experimental values and the predictions of EMT is clear (100% for the lowest frequency). As the value taken for the radius of the bubbles is certainly an upper limit, the frequencies are sure to be much lower than the lowest resonance frequency (3.9 kHz for a diethyl-ether bubble with a radius $R_0 = 1$ mm) and the volume fraction is in our experiments always less than 0.4%: under such experimental conditions it is known that the EMT correctly describes the behaviour of liquid/gas mixtures†. As a first result we experimentally demonstrate that the EMT is unable to account for the behaviour of liquid/vapour mixtures.

On the other hand, the predictions of MEMT are in good quantitative agreement with the experimental values; even in the part of the curve where the agreement seems poor, i.e., for f from 0.1% to 0.15% the discrepancy is always less than 10%.

4.2. *Width of the first resonance*

The position of the first resonance of the tube depends both on the phase velocity of the sound wave and on the attenuation. On the other hand, the width of the resonance curve depends only on the damping, that is on the attenuation of the wave: if the wave is not attenuated, there is no damping and only infinitely fine resonances of infinite amplitude. The comparison between the experimental width of the first resonance and the calculated one obtained from the EMT and the MEMT gives indications of the validity of the attenuation predicted by the respective models.

We measure the width of each curve at half-amplitude; in order to get the

† Silberman (1957) reports measurements at frequencies down to a few tens of Hz.

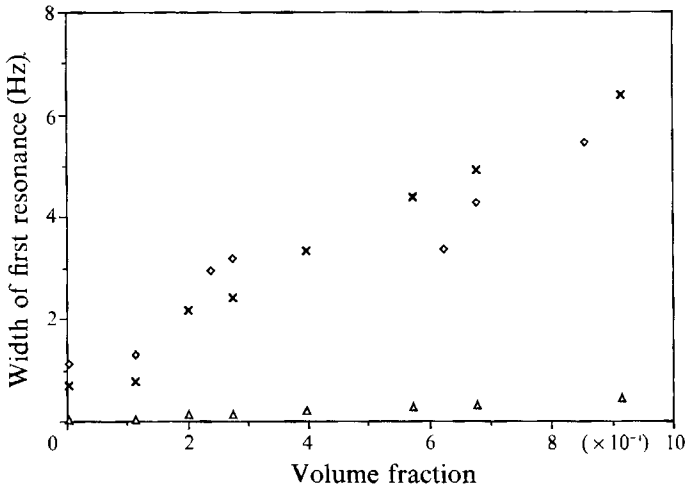

FIGURE 6. Evolution of the width of the first resonance with the volume fraction. A comparison is made between the experimental values (◇), the predictions of EMT (△) and those of the MEMT (×).

predictions of the two models, we use (3.10) and (3.9) with (3.6a) or (3.6b). We calculate numerically the maximum amplitude of the pressure, $P_{\max}$ and use this value to determine the width as the difference between the two numerical solutions of the equation $P_l(\nu) = \frac{1}{2}P_{\max}$.

The result of the comparison is shown on figure 6. On one hand, one sees that the predictions of the EMT do not agree with the measurements, even in order of magnitude as was the case for the position of the resonance: the greatest width predicted by the EMT is 0.5 Hz whereas the actual one is 5.6 Hz. This shows that the main failure of the EMT rests in the attenuation, which is underevaluated; the phenomenon responsible for sound attenuation is the dissipative transport in the liquid of the latent heat due to phase transition at the interface, rather than the damping of the bubble oscillations by the viscosity of the liquid and the thermal processes in the gas. On the other hand, the predictions of the MEMT agree quite well with the experimental values, showing that the dissipative phenomenon is correctly taken into account by this model.

4.3. *Position of the second resonance*

In principle, (3.9) gives the position of the higher resonances of the tube. We use to calculate the second resonance frequency for both the EMT and MEMT; the predictions of the EMT are displayed on figure 8 below and show a clear discrepancy with the observations.

When the calculations are done with the expression for t given by the MEMT, (3.6a), we find no resonance at all, i.e. the imaginary part of the input impedance is never zero, for any frequency in the range of interest. This result seems disappointing, but one should remember that there might be a local maximum in the plot of the pressure versus the frequency, without any actual resonance of the tube (i.e. in the sense corresponding to the definition of §3). We cannot employ (3.9) anymore and we have to use (3.10) to plot the calculated resonance curve and to compare it to the experimental one.

In figure 7(a) we show an experimental curve $P_l(\nu)$; the pressure at point $x = l$ is

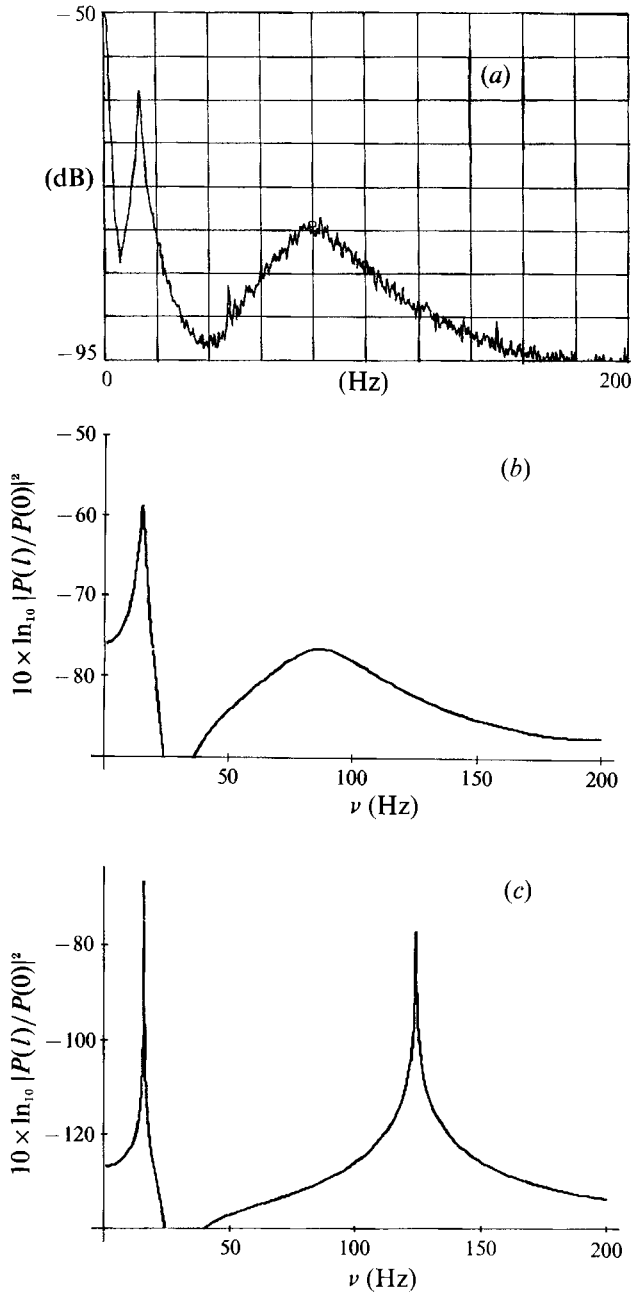

FIGURE 7. (*a*) A plot of the first two experimental resonances from measurements with a spectrum analyser; it is a power spectrum and the ordinate units are dBVrms. The spectrum is obtained after 47 averages. (*b*) As (*a*) but calculated with the MEMT. The structure is very reminiscent of that of the experimental plot; note also that the minimum of the curve is much deeper than the 'actual' one, since the contribution of other sources of damping that we have neglected becomes predominant. (*c*) As (*a*) but calculated with the EMT. The discrepancy with the experimental curve is obvious; note also that the resonances are sharper than they look, because of the numerical resolution. The first peak is calculated at ≈ -40 dB and the second one at ≈ -77 dB.

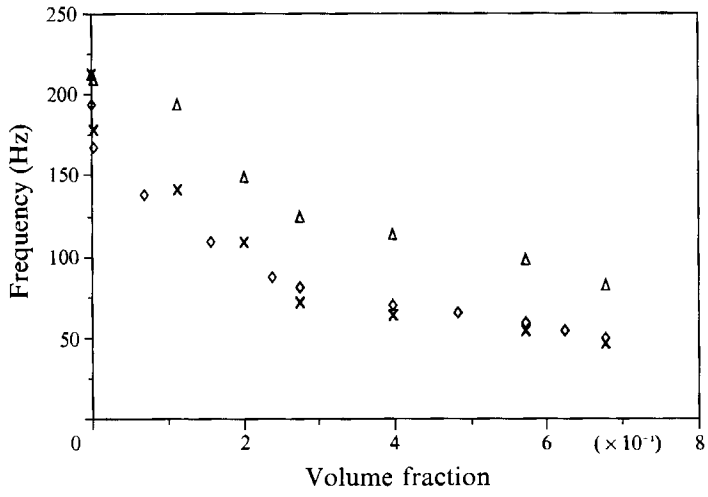

FIGURE 8. Evolution of the second resonance frequency with the volume fraction. The comparison is made between the experimental values (◇), the predictions of EMT (△) from (3.9) and those of the MEMT (×) from numerical determination of the second maximum of $P(\nu)$, according to (3.10).

measured with the upper pressure transducer (see figure 1). The obvious feature of this curve is the broadening of the second resonance; its width is about 30 Hz for a resonance frequency of 80 Hz whereas the width of the first peak is 1.7 Hz for a resonance frequency of 15.5 Hz. This is a strong indication that the two resonances do not correspond to the same physical effect. The theoretical curve calculated with the MEMT is displayed on figure 7 (*b*), and the curve given by the EMT on figure 7 (*c*). The analogy of structure between the experimental curve and the theoretical one obtained with the MEMT is striking: the second peak has a much lower amplitude and undergoes a considerable widening, both experimentally and in the calculations based on the MEMT. Thus the MEMT does predict a peak in the curve $P_l(\nu)$, but this peak does not correspond to an actual resonance of the tube.

In fact, the attenuation is too high for the second resonance to exist, and experimentally the only memory of the latter is a very wide peak; the MEMT succeeds very well in predicting that the imaginary part of the input impedance does not vanish anymore, i.e. there is no actual resonance, but that in place of it there appears a wide peak in the curve $P_l(\nu)$. On the other hand, the attenuation given by the EMT is too low to make the resonance disappear, and there is clearly a discrepancy between the form of the resonance curve and the experimental one. We emphasize the fact that the two models differ not only in numerical predictions, but also on the very structure of the resonance curve. Note also that this fact is consistent with the previous results on the width of the first resonance, which also show that the EMT underestimates the attenuation of the wave.

To calculate the predictions of the MEMT for the position of the second 'resonance' we calculate the second maximum of the curve $P_l(\nu)$ numerically because (3.9) is not verified. This method gives the results displayed in figure 8, which are in very good agreement with the observations.

4.4. *Amplitude of the resonances*

Our apparatus does not allow us to measure the pressure at the input of the tube, and the geometry of the piston makes difficult to deduce it from its acceleration. On the other hand the difference between the amplitudes of the first peak and of the second

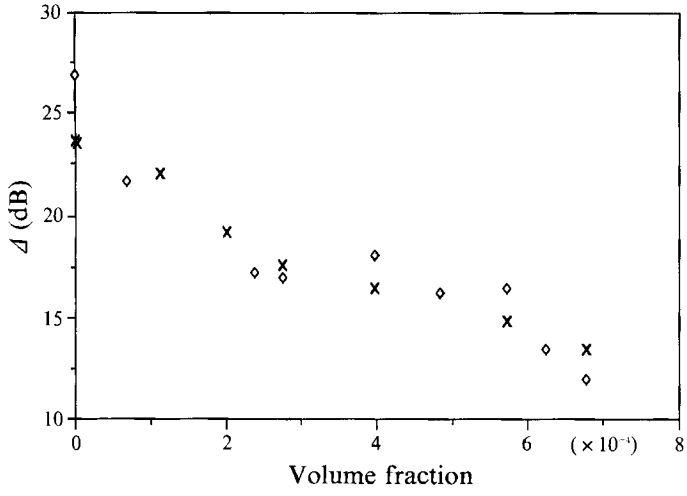

FIGURE 9. Evolution of the difference of amplitude between the two first peaks in the curve $P_l(\nu)$, in dBrms, with the volume fraction. The comparison is made between the experimental values (◇) and those of the MEMT (×).

one is easily accessible both experimentally and numerically, since the input pressure does not appear anymore. It is an interesting quantity related to the attenuation part of the propagation constant; the result of the comparison is shown in figure 9. Calculations are made only with the MEMT and show reasonable agreement with the experimental values. As the EMT fails to predict the positions of the resonances, we do not calculate the corresponding amplitudes; in fact the attenuation is so underevaluated that the first peak is much too sharp and high. In the case of figure 7, that is at $f \approx 2.7 \times 10^{-4}$, the measured difference between the two amplitudes in dBvrms is 17.5 dB, the prediction of EMT is 38.3 dB and that of MEMT is 18 dB.

5. Discussion

The results presented in the preceeding section establish without any doubt that the EMT is unable to describe the behaviour of a liquid/vapour mixture at low frequency and low volume fraction of vapour. The discrepancy between the EMT and the experiments for the quantities which depend almost only on the attenuation (the width of the first resonance curve in §4.2, the ratio of amplitude of the two first peaks in §4.4 and the structure of the second peak in §4.3) establishes that the main failure of this model consists in the underestimation of the dissipative phenomena causing the attenuation of the wave. Moreover, since the positions of the resonances do not agree with the experimental values, the phase velocity given by the EMT is probably incorrect also. This conclusion is a new experimental result showing the specific character of liquid/vapour mixtures. Note also that the most important limitation of our experiments, that is the lack of statistical knowledge of the bubble population, is without consequence because the only relevant parameter of the EMT is the volumic fraction of vapour, a global† quantity.

On the other hand, we give evidence that the MEMT does agree with our experiments: it gives with a good precision how the first resonance of the tube varies

† In fact, as is clear from (2.7), the imaginary part of the propagation constant depends explicitly on the mean bubble radius R_0 and is thus sensitive to polydispersity. However, the polydispersity is unable to explain discrepancies of several orders of magnitude.

with the volume fraction. The width of the first resonance is also well predicted by the MEMT. It indicates that the dissipative phenomenon of concern in liquid/vapour mixtures is correctly taken into account by the MEMT. Thirdly the MEMT displays the actually observed disappearance of the second resonance of the tube: only a broad peak remains, and the value of the peak frequency as well as the structure of the resonance curve are in good agreement with the observations. Finally, it predicts a ratio of the amplitudes of the first two peaks of the $P_i(\nu)$ curve which is very close to the actually observed one.

Nevertheless, there remains the experimental problem of the polydispersity of the bubble population. All our calculations are made with a monodisperse population of bubbles having a typical radius equal† to 1 mm. This value is consistent with visual observation, an argument which may seen extremely doubtful but which is strengthened by the fact that we use a unique parameter to analyse data which are of different types and in different frequency domains. Moreover we know that the radius of a bubble going away from a solid wall under the action of buoyancy forces (see e.g. Bikerman 1973, p. 54) is

$$R_0 \sim [\sigma/g(\rho_1-\rho_g)]^{\frac{1}{2}},$$

where σ is the surface tension and g the gravitational acceleration; this gives $R_0 \approx 1.5$ mm. This is of course only an order of magnitude, and the radius of a bubble leaving a capillary or a wall is still a difficult open problem, but it is nice to recover the same order of magnitude as the one that we observed.

Another question to ask is whether the theory itself should be independent of the polydispersity, despite the explicit presence of the bubble radius in the final formula. We investigate this possibility in a very simple way: we take a bidisperse population, with $N^{\flat}_{1,2}$ bubbles with radius $R_{1,2}$ and maintain the volume fraction of vapour fixed, so that

$$N^{\flat}_1 \tfrac{4}{3}\pi R_1^3 + N^{\flat}_2 \tfrac{4}{3}\pi R_2^3 = V_g = \text{const.} \tag{5.1}$$

We take $R_1 < R_2 = R_0$ because we expect R_0 to play the part of an upper limit for the bubble radius; in practice we discuss results with $R_1 = \frac{1}{2}R_2$ and $R_1 = \frac{1}{10}R_2$. Let $V_{1,2} \equiv N^{\flat}_{1,2}\frac{4}{3}\pi R^3_{1,2}$; at small volumic fraction $f \approx V_g/V_l$ and we define x as

$$V_1/V_l \equiv xf; \quad V_2/V_l \equiv (1-x)f; \tag{5.2}$$

then x is the only adjustable parameter along with $r \equiv R_2/R_1$; x ranges from 0 (only big bubbles) to 1 (only small ones). The next step is the generalization of (2.8) for a polydisperse population of bubbles; it is very simple if one follows the calculations of Onuki (1991). The (complex) effective compressibility K_{lv} reads

$$\rho K_{lv} = \frac{k^2}{\omega^2} = \frac{1}{c^2_{\text{eff}}} + \frac{m}{3\gamma p_0}\langle 1-\Theta\rangle_l \tag{5.3}$$

where ρ is the averaged density and m is the parameter defined in (2.9). $\langle 1-\Theta\rangle_l$ is the average over the disorder of the dimensionless temperature field Θ_l, on the liquid side. In the frequency range of interest, the temperature field around each bubble is independent of the other bubbles and the average is taken without any difficulty. The expression for Θ_l is (see equation 2.35b of the paper by Onuki 1991, where Θ is denoted F)

$$1-\Theta_l(u) = \frac{R_i}{u}\exp\left[\left(\frac{i\omega}{D_l}\right)^{\frac{1}{2}}(R_i-u)\right] \tag{5.4}$$

† It may be considered as a parameter whose value is obtained by fitting the experimental results with the predictions of the MEMT; the precision is about $\pm 10\%$.

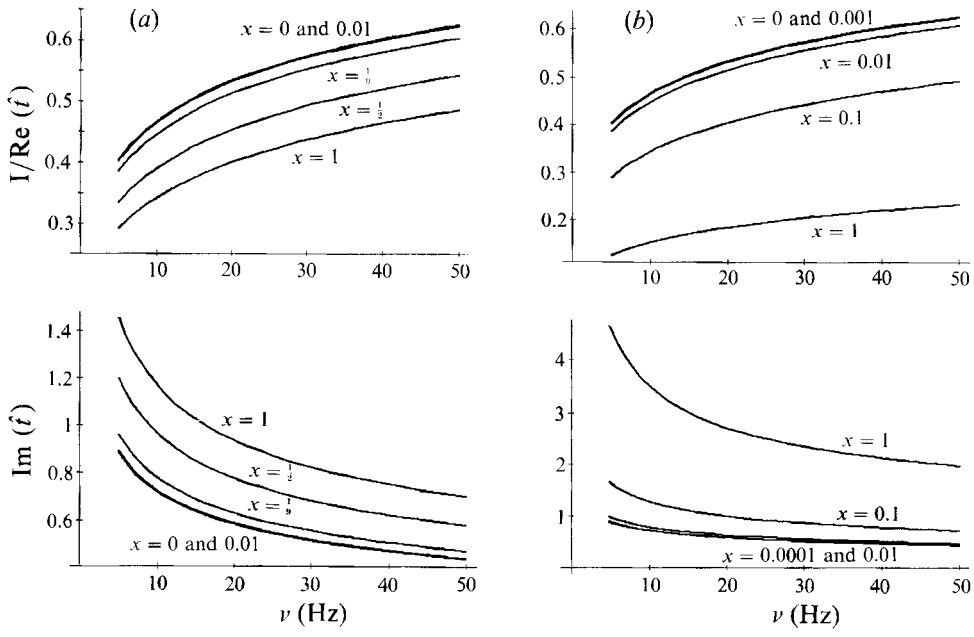

FIGURE 10. Plot of the dimensionless phase velocity $[1/\mathrm{Re}\,(\hat{f})]$ and attenuation $[\mathrm{Im}\,(\hat{f})]$ versus the frequency for a mixture of bubbles with radii (*a*) $R_2 = 1$ mm and $R_1 = 0.5$ mm, and (*b*) $R_2 = 1$ mm and $R_1 = 0.1$ mm.

where u is the radial coordinate, with the origin taken at the centre of the bubble. Then we get

$$\langle 1-\Theta\rangle_1 \equiv \frac{\int_{V_1} \mathrm{d}u(1-\Theta_1)}{V_1} = \frac{N_1^{\mathrm{b}}}{V_1}\int_{R_1}^{\infty} 4\pi u^2\,\mathrm{d}u(1-\Theta_1) + \frac{N_2^{\mathrm{b}}}{V_1}\int_{R_2}^{\infty} 4\pi u^2\,\mathrm{d}u(1-\Theta_1)$$

$$\approx 3f\left[\frac{rx}{(\mathrm{i}\omega\tau_1)^{\frac{1}{2}}}\left(1+\frac{r}{(\mathrm{i}\omega\tau_1)^{\frac{1}{2}}}\right)+(1-x)\frac{1}{(\mathrm{i}\omega\tau_1)^{\frac{1}{2}}}\right], \tag{5.5}$$

where we have used $\tau_1 \equiv R_2^2/D_1$; we have also kept the term proportional to $1/\omega$ because it cannot be neglected for small bubble radius (e.g. for $r = 10$; note that this term is neglected in (2.8), which is legitimated by the value of R_0). We thus get the corrected expression for the propagation constant:

$$k = \frac{\omega}{c_\phi} - \mathrm{i}\alpha_\phi = \frac{\omega}{c_{\mathrm{eff}}}\left\{1+[1+x(r-1)](1+\mathrm{i})\frac{m}{(2\omega\tau_1)^{\frac{1}{2}}}+\mathrm{i}xr^2\frac{m}{\omega\tau_1}\right\}^{\frac{1}{2}} \tag{5.6}$$

The term that is the factor of $(\omega/c_{\mathrm{eff}})$ on the right-hand side is hereafter noted $\hat{t}$ because it is a generalization of the term t defined in (3.6). We can study the evolution of the dimensionless phase velocity $1/\mathrm{Re}\,(\hat{t})$ and of the attenuation $\mathrm{Im}\,(\hat{t})$ when x varies, for a given r. The results are displayed in figure 10 for $r = 2$ (figure 10*a*) and $r = 10$ (figure 10*b*). They differ by no more than a few percent even when there are as many small bubbles as big ones for $r = 2$ ($x = \frac{1}{9}$), and when the small bubbles are ten times as numerous (such a proportion should not escape even simple observation) as the big ones for $r = 10$ ($x = 0.01$). Thus the phase velocity and attenuation are not very sensitive to the polydispersity; in fact, it seems that the mixture behaves as if the bubbles which contribute mostly to the volume fraction were alone.

On the other hand, as is clear from §4, our measurements are indirect determinations of both the phase velocity and the attenuation, and this causes a lack in sensitivity. Both this experimental limitation and the feature of the theory described above may explain why our measurements are in good agreement with the predictions of the MEMT, despite the polydispersity of the bubble population.

We acknowledge support from the DRET under contract 89/1482. We thank E. Wolf for useful discussions and S. Fauve for careful reading of the manuscript. We also thank the referees for useful comments.

REFERENCES

Ardron, K. H. & Duffey, R. B. 1978 Acoustic wave propagation in a flowing liquid–vapour mixture. *Intl J. Multiphase Flow* **4**, 303–322.

Bikerman, J. J. 1973 *Foams*. Springer.

Boguslavski, Yu. Ya. 1978 Absorption and dispersion of sound waves in two-phase medium. *Sov. Phys. Acoust.* **24**, 24–27.

Borisov, A. A., Borisov, Al. A., Kutateladze, S. S. & Nakoriakov, V. E. 1983 Rarefaction shock wave near the critical liquid–vapour point. *J. Fluid Mech.* **126**, 59–73.

Cartensen, E. L. & Foldy, L. L. 1947 Propagation of sound through a liquid containing bubbles. *J. Acoust. Soc. Am.* **19**, 481–501.

Commander, K. W. & Prosperetti, A. 1989 Linear pressure waves in bubbly liquids: comparison between theory and experiments. *J. Acoust. Soc. Am.* **85**, 732–746.

Coste, C. 1991 Propagation d'ondes acoustiques dans les mélanges diphasiques liquide/vapeur. PhD thesis, Université Claude Bernard, Lyon.

Coste, C., Laroche, C. & Fauve, S. 1990 Sound propagation in a liquid with vapour bubbles. *Europhys. Lett.* **11**, 343–347.

Devin, C. 1959 Survey of thermal, radiation and viscous damping of pulsating air bubbles in water. *J. Acoust. Soc. Am.* **31**, 1654–1667.

Feldman, C. L., Nydick, S. E. & Kokernak, R. P. 1972 The speed of sound in single-component two-phase fluids: theoretical and experimental. *Prog. Heat Mass Transfer* **6**, 671–684.

Finch, R. D. & Neppiras, E. A. 1973 Vapor bubble dynamics. *J. Acoust. Soc. Am.* **53**, 1402–1410.

Hsieh, D. Y. 1979 On oscillation of vapor bubbles. *J. Acoust. Soc. Am.* **66**, 1514–1515.

Hsieh, D. Y. 1982 Some aspects of dynamics of bubbly liquids. *Appl. Sci. Res.* **38**, 305–312.

Kieffer, S. W. 1977 Sound speed in liquid–gas mixtures: water–air and water–steam. *J. Geophys. Res.* **82**, 2895–2903.

Kinsler, L. E., Frey, A. R., Coppens, A. B. & Sanders, J. V. 1982 *Fundamentals of Acoustics*. Wiley.

Kokernak, R. P. & Feldman, C. L. 1972 Velocity of sound in two-phase flow of R12. *American Society of Heating, Refrigerating and Air Conditioning Engineers J.* **14**, 35–38.

Kutateladze, S. S., Nakoriakov, V. E. & Borisov, A. A. 1987 Rarefaction waves in liquid and gas-liquid media. *Ann. Rev. Fluid Mech.* **19**, 577–600.

Landau, L. & Lifshitz, E. 1959 Sound waves. In *Fluid Mechanics*, §64. Pergamon.

Mallock, A. 1910 The damping of sound by frothy liquids. *Proc. R. Soc. Lond.* A **84**, 391–395.

Marston, P. L. 1979 Evaporation-condensation resonance frequency of oscillating vapor bubbles. *J. Acoust. Soc. Am.* **66**, 1515–1521.

Mecredy, R. C. & Hamilton, L. J. 1972 The effect of nonequilibrium heat, mass and momentum transfer on two-phase sound speed. *Intl J. Heat Mass Transfer* **15**, 61–72.

Mecredy, R. C., Wigdortz, J. M. & Hamilton, L. J. 1970 Prediction and measurement of acoustic wave propagation in two-phase media. *Trans. Am. Nucl. Soc.* **13**, 672–673.

Minnaert, M. 1933 On musical air bubbles and the sound of running water. *Phil. Mag.* **XVI**, 235–248.

Morse, P. M. & Ingard, K. U. 1986 *Theoretical Acoustics*. Princeton University Press.

NAKORIAKOV, V. E., POKUSAEV, B. G. & SCHREIBER, I. R. 1980 Pressure waves in a liquid with gas or vapour bubbles. In *Cavitation and Inhomogeneities* (ed. W. Lauterborn), pp. 157–163. Springer.

NAKORIAKOV, V. E., POKUSAEV, B. G., PRIBATURIN, N. A. & SCHREIBER, I. R. 1984 Acoustics of a liquid containing vapour bubbles. *Sov. Phys. Acoust.* **30**, 480–482.

NIGMATULIN, R. I. 1991 *Dynamics of Multiphase Media*. Hemisphere.

NIGMATULIN, R. I., KHABEEV, N. S. & ZUONG NGOK HAI 1988 Waves in liquids with vapour bubbles. *J. Fluid Mech.* **186**, 85–117.

ONUKI, A. 1991 Sound propagation in phase-separating fluids. *Phys. Rev.* A **43**, 6740–6755.

PLESSET, M. S. & PROSPERETTI, A. 1977 Bubble dynamics and cavitation. *Ann. Rev. Fluid Mech.* **9**, 145–185.

PLESSET, M. S. & ZWICK, S. A. 1954 The growth of vapor bubbles in superheated liquids. *J. Appl. Phys.* **25**, 493–500.

PROSPERETTI, A. 1977 Thermal effects and damping mechanisms in the forced radial oscillations of gas bubbles in liquids. *J. Acoust. Soc. Am.* **61**, 17–27.

PROSPERETTI, A. 1991 The thermal behaviour of oscillating gas bubbles. *J. Fluid Mech.* **222**, 587–616.

SILBERMAN, E. 1957 Sound velocity and attenuation in bubbly mixtures measured in standing wave tubes. *J. Acoust. Soc. Am.* **29**, 925–933.

TEMKIN, S. 1990 Attenuation and dispersion of sound in bubbly fluids via the Kramers–Kronig relations. *J. Fluid Mech.* **211**, 61–72.

TRAMMEL, G. T. 1962 Sound waves in water containing vapour bubbles. *J. Appl. Phys.* **33**, 1662–1670.

WANG, T. 1974 Effect of evaporation and diffusion on an oscillating bubble. *Phys. Fluids* **17**, 1121–1126.